Structural and Thermal Characterization of Poly(2-chloroaniline)/Red Mud Nanocomposite Materials

Ayşegül Gök, İsa Oğuz

Department of Chemistry, Faculty of Arts and Science, Süleyman Demirel University, 32260 Isparta, Turkey

Received 5 January 2005; accepted 3 May 2005
DOI 10.1002/app.22740
Published online 6 December 2005 in Wiley InterScience (www.interscience.wiley.com).

ABSTRACT: We report the synthesis and characterization of a series of conducting poly(2-chloroaniline) (P2ClAn)/red mud (RM) nanocomposite materials. The polymerization of 2-chloroaniline in an aqueous medium in the presence of $(NH_4)_2S_2O_8$ and RM resulted in the formation of a nanocomposite (P2ClAn/RM). The extent of P2ClAn loading in the composites increased with increasing oxidant and monomer concentrations but decreased with RM. The properties of the nanocomposites were characterized with Fourier transform infrared (FTIR), ultraviolet–visible (UV–vis), conductivity measurements, scanning electron microscopy, thermogravimetric analysis, and differential scanning calorimetry analysis. The inclusion of P2ClAn in the composites was confirmed by FTIR studies. The UV–vis spectra of P2ClAn/RM nanocomposites were similar to that of P2ClAn. The conductivity changed in all the composites prepared under various conditions. Thermogravimetric analyses revealed the enhanced thermal stabilities of the nanocomposites with respect to P2ClAn. Morphological images of the as-synthesized materials were also investigated with scanning electron microscopy and environmental scanning electron microscopy. © 2005 Wiley Periodicals, Inc. J Appl Polym Sci 99: 2101–2108, 2006

Key words: conducting polymers; morphology; nanocomposites

INTRODUCTION

Recently, polymer-based nanocomposite materials have evoked extensive research interest because of their unique characteristics in the creation of potential commercial applications. The introduction of an organic guest into an inorganic host material by the intercalation technique has resulted in the fabrication of nanocomposite materials with high potential for advanced electronic,[1] magnetic,[2] optical,[3] and chemical sensing applications.[4] The combination of conducting polymers with host materials having different characteristics opens a way to new hybrid materials showing novel properties.[5,6] Clays, among other hosts, are natural, abundant, and inexpensive minerals that have a unique layered structure, high mechanical strength, and high chemical resistance. Nanocomposite materials have been reported to boost the thermal stability,[7] mechanical strength,[8] and molecular-barrier,[9] flame-resistance,[10] and corrosion-inhibition properties[11] of polymers by incorporating small amounts of clay platelets into the polymer matrix.

Most recently, as one of the most intensively studied conducting polymers in the last 15 years, polyaniline has attracted considerable attention for the preparation of its composites with host particles, such as conducting polyaniline/CdS and polyaniline/Cu_2S,[12] polyaniline/clay,[13] polyaniline/V_2O_5,[14] and polyaniline–dodecylbenzenesulfonic acid (DBSA)/organophilic clay[15] nanocomposite systems. However, polyaniline has always been regarded as an intractable material because of its poor solubility in common organic solvents. Many soluble derivatives of polyaniline are therefore synthesized by the polymerization of ring- or nitrogen-substituted aniline monomers and/or by polymerization.[16,17] Among these derivatives, poly(*o*-methoxyaniline) has attracted much attention because of its better solubility.[18] However, its conductivity is much lower than that of polyaniline.

Although composites of poly(2-chloroaniline) (P2ClAn), which is a halogen-substituted polyaniline, are reported in the literature,[19,20] fewer reports seem to be available dealing with P2ClAn nanocomposites, including the nanostructure. In this study, we prepared a series of P2ClAn/red mud (RM) nanocomposite materials by effectively dispersing the inorganic nanolayers of RM in an organic P2ClAn matrix through in situ oxidative polymerization. Moreover, the preparation of P2ClAn/RM nanocomposites with RM is interesting for the evaluation of RM. The characterization of as-prepared P2ClAn/RM composites included electrical-conductivity measurements, Fourier transform infrared (FTIR) and ultraviolet–visible (UV–vis) spectroscopy, thermogravimetric analysis

Correspondence to: A. Gök (aysegul@fef.sdu.edu.tr).
Contract grant sponsor: Suleyman Demirel University Research Fund; contract grant number: 03-M-736.

TABLE I
Some Typical Data For P2C1An/RM [$(NH_4)_2S_2O_8$] Polymerization/Composite Formation

Entry	Compound code	Weight of RM (g)	Oxidant $\times 10^3$ (mol)	2ClAn $\times 10^3$ (mol)	Time of polymerization (h)	Yield of P2ClAn (wt %)	P2ClAn/g of composite (wt %)	Conductivity (S/cm^{-1})
1	P2ClAn	—	17.49	8.76	24	18.95	—	9.43×10^{-5}
2	P2ClAn/RM 1	0.1	8.74	8.76	24	4.68	34.30	2.59×10^{-5}
3	P2ClAn/RM 2	0.1	17.49	8.76	24	12.00	58.00	3.71×10^{-5}
4	P2ClAn/RM 3	0.1	26.23	8.76	24	20.84	69.93	5.44×10^{-5}
5	P2ClAn/RM 4	0.1	34.97	8.76	24	19.88	69.94	5.08×10^{-5}
6	P2ClAn/RM 5	0.2	17.49	8.76	24	8.98	33.38	3.57×10^{-5}
7	P2ClAn/RM 6	0.3	17.49	8.76	24	8.12	23.20	2.56×10^{-5}
8	P2ClAn/RM 7	0.4	17.49	8.76	24	5.51	13.33	2.40×10^{-5}
9	P2ClAn/RM 8	0.1	17.49	4.38	24	3.19	15.11	1.21×10^{-5}
10	P2ClAn/RM 9	0.1	17.49	6.57	24	11.64	49.34	1.34×10^{-5}
11	P2ClAn/RM 10	0.1	17.49	13.14	24	99.37	94.33	5.05×10^{-5}

(TGA), differential scanning calorimetry (DSC), scanning electron microscopy (SEM), and environmental scanning electron microscopy/field emission gun (ESEM–FEG).

EXPERIMENTAL

Materials

2-Chloroaniline (2ClAn) monomer (Aldrich, Milwaukee, WI; 99.5% pure) was distilled under reduced pressure. RM was supplied by the Etibank Seydişehir Aluminum Plant (Konya, Turkey) and had the following average composition (wt %): Al_2O_3, 18.71 ± 0.59; Fe_2O_3, 39.70 ± 0.67; TiO_2, 4.90 ± 0.54; Na_2O, 8.82 ± 0.96; CaO, 4.47 ± 0.56; and SiO_2, 14.52± 0.37 (the loss on ignition was 8.15 ± 0.40).[21] The original RM was prepared via washing with HCl and water until neutralization and then was dried. RM was dried in vacuo at 100°C for 3 days before use in each experiment. HCl, $(NH_4)_2S_2O_8$, and 1-methyl-2-pyrrolidinone (NMP) were analytical-reagent-grade and were used without further purification.

Synthesis

In a typical procedure, 1 mL of distilled *o*-chloroaniline (8.76 mmol) was dissolved in 100 mL of 1.0*M* HCl. A solution of $(NH_4)_2S_2O_8$ (17.46 mmol) in 1.0*M* HCl was added to the 2ClAn solution dropwise over a period of 30 min with vigorous magnetic stirring at 25°C. After about 24 h, the precipitate was collected in a Buchner funnel. Upon drying in vacuo, HCl-doped P2ClAn was obtained as a green powder.

The P2ClAn/RM composite was prepared as follows. A known weight of RM was added to a solution of 1.0*M* HCl. Then, 1 mL of 2ClAn was added, and the mixture was stirred for 4 h at 25°C. To this dispersion, a known volume of an $(NH_4)_2S_2O_8$ solution was added, and the polymerization lasted for 24 h. The separated mass was repeatedly washed with an HCl solution and water and finally dried in a vacuum oven at 70°C for 24 h.

Characterization

The direct-current conductivity measurements were conducted on pressed pellets by a four-probe technique. FTIR spectra were taken on a PerkinElmer BX model instrument (Buckinghamshire, UK). The UV–vis spectra were obtained on a PerkinElmer λ 20 model spectrophotometer. The thermal stability of P2ClAn and its nanocomposites with RM was investigated with a PerkinElmer thermal parametric analyzer with pure nitrogen gas at a flow rate of 35 mL/min. The heating rate was 10°C/min. DSC analysis was performed on a DuPont General V4.1C 2000 analyzer (Wilmington, DE). The microstructure of the materials was imaged through a JEOL 5600-LV SEM instrument (Tokyo, Japan). Particle diameter analysis was performed with a Philips model XL30 ESEM–FEG instrument operating at 10 kV in a low vacuum. The sample was mounted on a double-sided, silver cohesive sheet; no gold coating was needed.

RESULTS AND DISCUSSION

General features of composite formation

Table I presents some results for the nanocomposite preparation involving P2ClAn with RM. The data (entries 2–5, Table I) suggest the formation of P2ClAn with an increasing amount of the oxidant, which is the usual and expected trend. Entries 3 and 6–8 of Table I further suggest a fall in the P2ClAn conversion corresponding to an increase in the RM concentration at fixed oxidant and 2ClAn concentrations. A similar situation was observed for a polypyrrole/Al_2O_3 nanocomposite system.[22] This is reasonable because, in the presence of RM as a heterogeneous surface, the

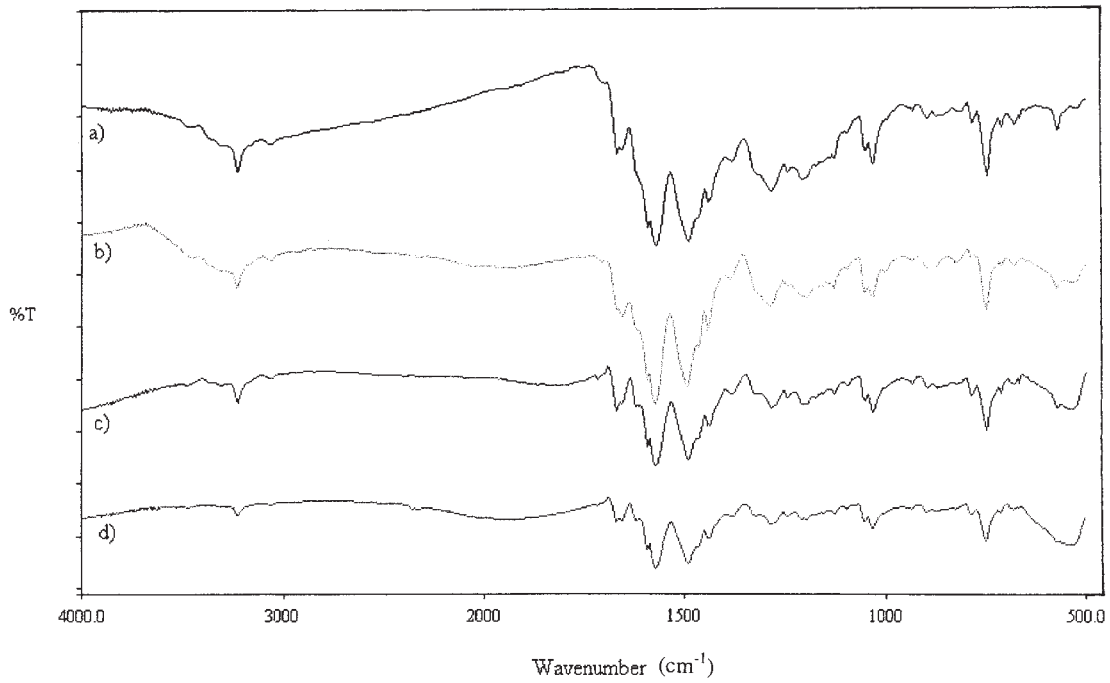

Figure 1 FTIR spectra of (a) P2ClAn, (b) P2ClAn/RM 9, (c) P2ClAn/RM 5, and (d) P2ClAn/RM 7.

P2ClAn oxidation reaction might be somewhat discouraged. For entries 3 and 9–11 of Table I, the conversion to P2ClAn increased with a higher 2ClAn concentration. The increase in the loading percentage of P2ClAn per gram of the composite was parallel to the increasing yield percentage of P2ClAn.

FTIR analysis

The FTIR spectra of P2ClAn and P2ClAn/RM composites are given in Figure 1. The characteristic vibration bands of P2ClAn are at 1286 (C—N stretching), 1573–1493 (N—H bending), and 3227 cm^{-1} (N—H stretching)[23] [Fig. 1(a)].

The incorporation of conducting polymer moieties into the respective polymer/nanostructure composites may be endorsed by FTIR spectral analysis.[24,25] FTIR spectra [Fig. 1(b–d)] of composites of P2ClAn indicate peaks of both P2ClAn and RM. In the FTIR spectra of P2ClAn/RM nanocomposites, the 500- and 536-cm^{-1} bands are the characteristic vibrations of RM,[26] and the 1493-, 1573-, and 1286-cm^{-1} bands are

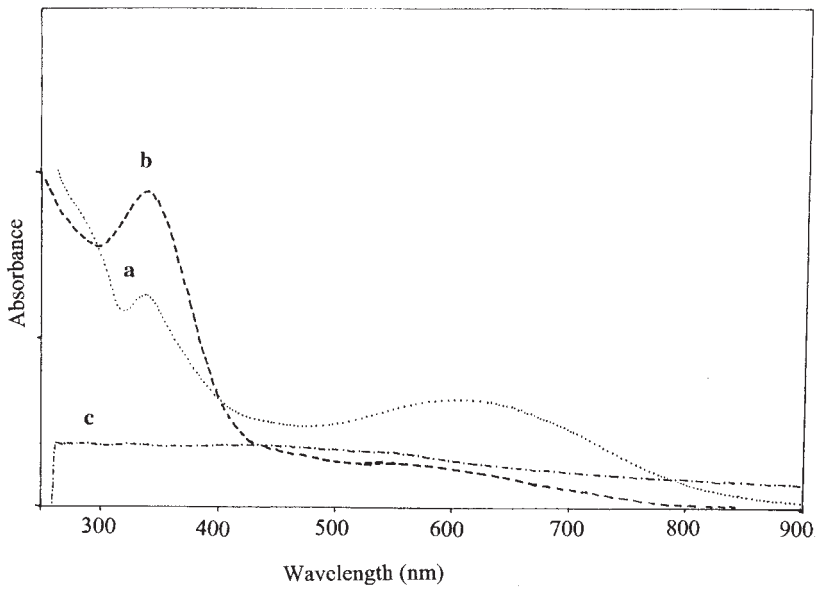

Figure 2 UV–vis spectra of (a) P2ClAn, (b) P2ClAn/RM 6, and (c) RM.

TABLE II
Maximum Absorbance Wavelengths of the P2ClAn and P2ClAn/RM Composites

Polymer	P2ClAn/g of composite (wt %)	λ_1 (nm) $\pi \rightarrow \pi^*$	λ_2 (nm) $n \rightarrow \pi^*$
P2ClAn	—	348	606
P2ClAn/RM 1	34.30	349	556
P2ClAn/RM 2	58.00	346	606
P2ClAn/RM 3	69.93	345	564
P2ClAn/RM 4	68.94	349	564
P2ClAn/RM 5	33.38	350	565
P2ClAn/RM 6	23.20	348	570
P2ClAn/RM 7	13.33	349	573
P2ClAn/RM 10	94.33	347	574

the characteristic vibrations of emeraldine salt.[27] The absorption peaks of the P2ClAn/RM 5 composite shifted to 1571 and 1198 cm^{-1}, whereas the characteristic absorption bands of P2ClAn are 1573 (N═Q═N) and 1211 cm^{-1} (C—N). As the loading of RM increased, the intensities of the characteristic bands of P2ClAn decreased; the stronger intensities of the RM vibration bands, especially the band at 526 cm^{-1}, can be found in the FTIR spectra of P2ClAn/RM materials in Figure 1(b–d).

UV–vis analysis

UV–vis spectra of P2ClAn, the P2ClAn/RM 6 composite, and RM were measured in NMP, as shown in Figure 2(a–c). The UV–vis spectrum of the doped P2ClAn has two major absorptions around 347 nm, which are related to the $\pi \rightarrow \pi^*$ transition on the polymer chain and the absorption at the wavelength longer 606 nm, which is contributed to the polaron after doping and corresponds to localization of the electron.[28] The UV–vis spectra in Figure 2 show a similarity between the P2ClAn/RM composites and P2ClAn polymer. The peak of the parent P2ClAn around 606 nm is based on the $n \rightarrow \pi^*$ transition of the quinone ring, whereas the peak of the P2ClAn/RM composites shift to a shorter wavelength (Table II).

These results indicate that there are some interactions between RM particles and P2ClAn.[29] RM did not show an absorption band at 250–800 nm [Fig. 2(c)].

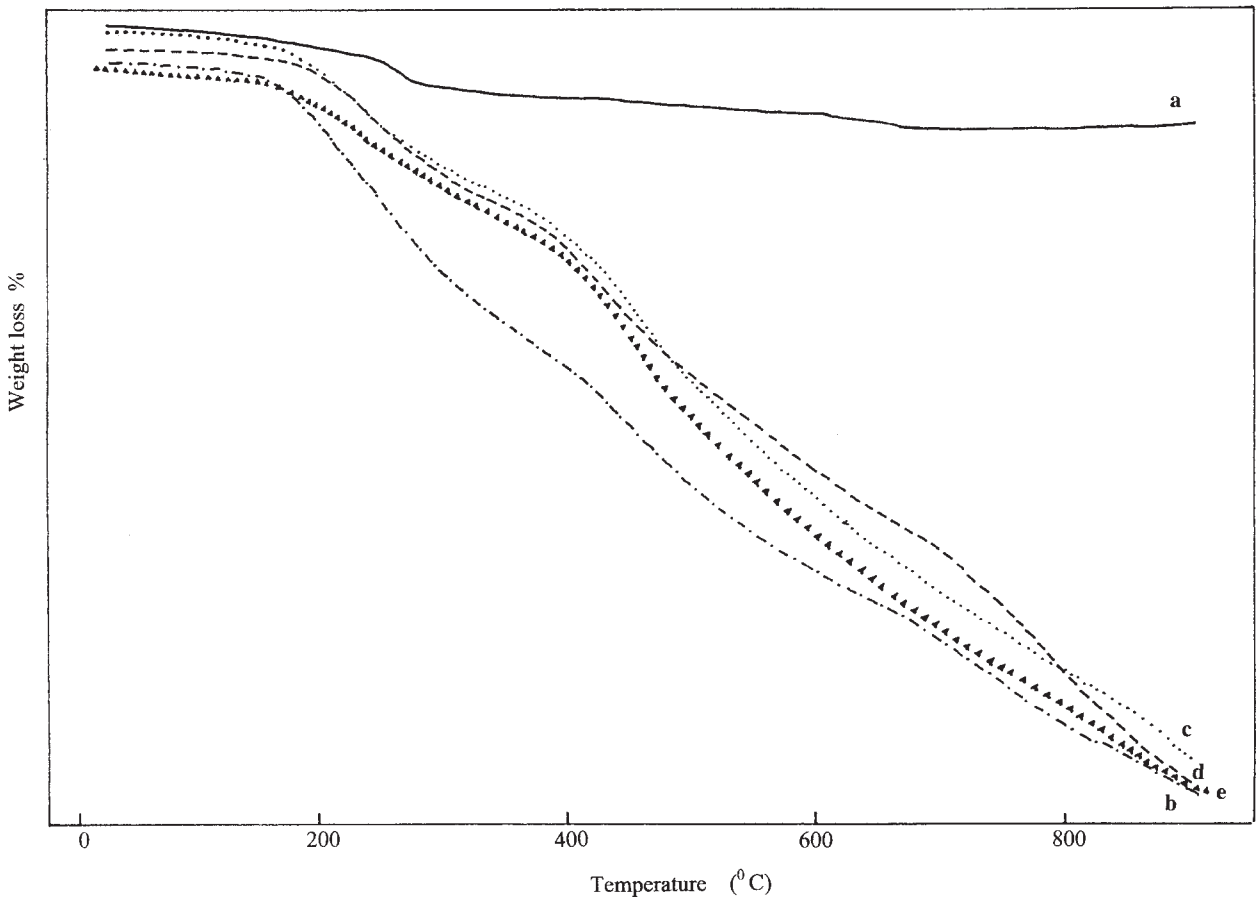

Figure 3 TGA thermograms of (a) RM, (b) P2ClAn, (c) P2ClAn/RM 1, (d) P2ClAn/RM 2, and (e) P2ClAn/RM 9.

TABLE III
TGA Results

Polymer	P2ClAn/g of composite (wt %)	T_i (°C)	T_m (°C)	T_f (°C)	Residue (wt %)
RM	—	246	261	272	89
P2ClAn	—	169	235	305	38
		429	500	563	
P2ClAn/RM 1	34.30	193	289	383	40
		383	441	500	
P2ClAn/RM 2	58.00	174	285	400	43
		400	476	546	
P2ClAn/RM 3	69.93	178	224	270	28
		409	483	570	
P2ClAn/RM 4	68.94	174	207	267	22
		400	476	530	
P2ClAn/RM 5	33.38	170	228	300	32
		391	430	470	
P2ClAn/RM 6	23.20	170	272	391	40
		391	433	476	
P2ClAn/RM 7	13.33	181	220	269	52
		400	433	459	
P2ClAn/RM 8	15.11	183	215	258	20
		676	733	795	
P2ClAn/RM 9	49.34	176	300	420	37
		420	450	483	
		483	565	650	
P2ClAn/RM 10	94.33	176	222	259	17
		380	530	693	

T_i = initial degradation temperature; T_m = maximum degradation temperature; T_f = final degradation temperature; Residue = nondegradation amount.

TGA results

Figure 3(a–e) presents typical weight-loss-temperature data for RM, P2ClAn, and P2ClAn/RM composites. Figure 3(c–e) shows typical TGA thermograms of the weight loss as a function of the temperature for P2ClAn/RM 1, P2ClAn/RM 2, and P2ClAn/RM 9 composites along with P2ClAn, as measured under an nitrogen atmosphere. Table III compares the thermal stabilities of RM, P2ClAn, and all the P2ClAn/RM composites. Although P2ClAn has 38% residue at 900°C, RM is more stable, with 89% residue at 900°C. RM suffers an 11% weight loss at 900°C because of the probable loss of volatile impurities.

TGA of P2ClAn and its composites indicates generally three stages of weight loss. The first weight loss (~2%) below 100°C is a result of the release of free water (this step is not shown in Table III). The weight losses in the temperature ranges of 169–193°C and 383–483°C can be attributed mainly to the dopant loss[30] and the subsequent structural decomposition of the polymer backbones at higher temperatures.[31] The increase in the thermal stabilities of the P2ClAn/RM composites can be seen in either the initial degradation temperatures or the residue values (%) with decreasing P2ClAn. Thus, these data confirm the enhanced thermal stability of the P2ClAn/RM composites with respect to that of P2ClAn.

DSC analysis

The DSC curves of P2ClAn, RM, and the P2ClAn/RM 5 composite are shown in Figure 4(a–c). The temperatures corresponding to transitions obtained from this curves are given in Table IV. The endothermic transitions can be seen in all the polymers. The endothermic peaks between 148 and 170°C in the DSC curves of P2ClAn and its composites can be attributed to dopant loss.[32] Two endothermic peaks in the DSC curve of RM can be seen at 292 and 372°C because of volatile matter. The DSC curves of the composites show endothermic peaks for both P2ClAn and RM. The transition temperatures in endothermic peak 2 are generally shifted to lower temperatures with RM entering the structure, and these temperature values are between the values of P2ClAn and RM. These results indicate that both P2ClAn and RM are in the composite structures. The second endothermic temperature in the composites can be attributed to the decomposition yields of P2ClAn removed from the RM structure.

Conductivity results

The electrical conductivity of the freestanding P2ClAn/RM composites was measured with the four-probe technique. The direct-current conductivity values (Table I) of the P2ClAn/RM composites increased

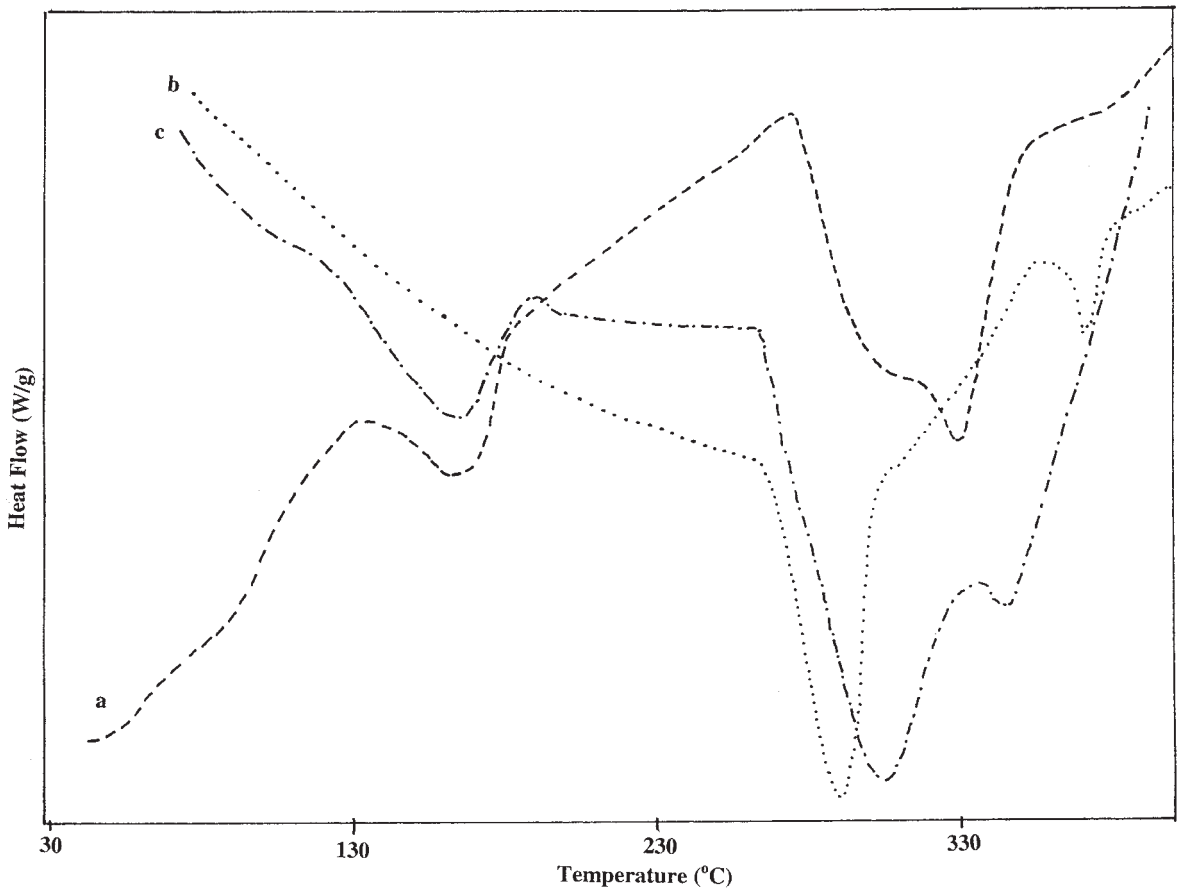

Figure 4 DSC curves of (a) P2ClAn, (b) RM, and (c) P2ClAn/RM 5.

(entries 2–11) with an increasing polymer loading in the composites. The conductivities of the P2ClAn/RM composites increased steadily with an increasing amount of the oxidant in the initial charge (entries 2–5, Table I). Both the overall poly(2-chloroaniline) yield and the P2ClAn loading per gram of the composite increased with the amount of the oxidant. Moreover, the electrical conductivity of all the P2ClAn/RM composites was smaller than that of P2ClAn, as shown in Table I. This was expected because the RM component is not electrically conductive and the incorporation of RM into the P2ClAn matrix contributes to the decrease in the electrical conductivity. Similar results were obtained in some similar works in the literature.[33,34]

TABLE IV
DSC Analysis Results

Polymer	P2ClAn/g of composite (wt %)	Endothermic peak 1	Endothermic peak 2	Endothermic peak 3
RM	—	—	291	372
P2ClAn	—	165	328	—
P2ClAn/RM1	34.30	170	309	346
P2ClAn/RM2	58.00	165	312	349
P2ClAn/RM3	69.93	165	311	347
P2ClAn/RM4	68.94	148	305	348
P2ClAn/RM5	33.38	167	304	347
P2ClAn/RM6	23.20	170	325	346
P2ClAn/RM7	13.33	170	316	347
P2ClAn/RM8	15.11	170	313	348
P2ClAn/RM9	49.34	165	318	346
P2ClAn/RM10	94.33	148	308	347

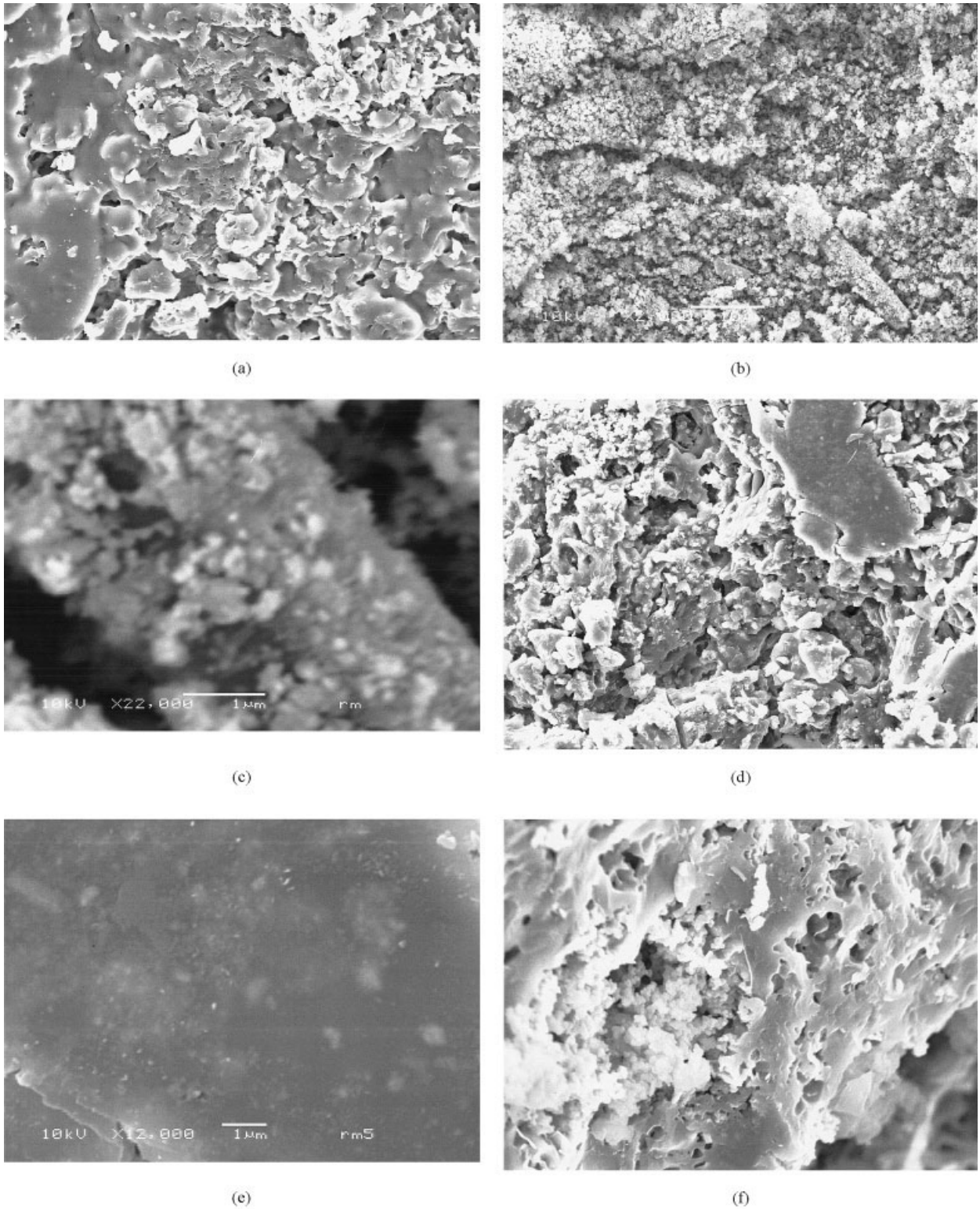

Figure 5 SEM micrographs of (a) P2ClAn (original magnification = 2000×, bar = 10 μm), (b) RM (original magnification = 2000×, bar = 10 μm), (c) RM (original magnification = 22,000×, bar = 1 μm), (d) P2ClAn/RM 5 (original magnification = 2000×, bar = 10 μm), (e) P2ClAn/RM 5 (original magnification = 12,000, bar = 1 μm), and (f) P2ClAn/RM 9 (original magnification = 2000×, bar = 10 μm).

Image analysis results

Figure 5 presents SEM images of P2ClAn, RM (2000 and 22,000×), and P2ClAn/RM 5 (2000 and 22,000×) and P2ClAn/RM 9 composites. In Figure 5(a), the morphology of P2ClAn is shown to be large layers with particles. The SEM micrograph of RM shows a

Figure 6 ESEM imagine of P2ClAn/RM 9.

structure with granules, including tiny spheres [Fig. 5(b,c)]. The average size of the particles is 100–150 nm. In general, SEM images of the P2ClAn/RM composites, including different amounts of P2ClAn per gram prepared in any medium, show the formation of irregular particles (both spherical and nonspherical), including some dusters [Fig. 5(d,f)]. The surface morphology of P2ClAn/RM 9, including much more P2ClAn, is similar to that of P2ClAn. P2ClAn/RM 5 exhibits relatively small, fine particles with respect to P2ClAn/RM 9. The reduction in the particle size of P2ClAn/RM 5 can be attributed to the heterogeneous nucleation effect of the dispersing RM in the polymeric matrix.[35] When the SEM image of P2ClAn/RM 5 is investigated at a higher magnification, both P2ClAn and RM structures can be seen [Fig. 5(e)]. P2ClAn/RM 9 was also characterized with environmental scanning electron microscopy (ESEM), as shown in Figure 6. The ESEM analysis showed that the nanocomposite consisted of aggregates, including particles of different dimensions (between 300 and 900 nm).

CONCLUSIONS

A series of P2ClAn/RM nanocomposites with different P2ClAn contents were prepared by an in situ intercalation/polymerization method. The conductivities of these composites were increased by increases in the loading of P2ClAn in the composite by various amounts of 2ClAn or an oxidant in the initial feed. The TGA results confirmed the enhanced thermostability in N_2 (g) of the P2ClAn/RM composites with respect to that of P2ClAn because of P2ClAn intercalation.

We believe that conducting nanocomposite polymers and materials will play important roles in intelligent materials science in the near future.

References

1. Yonoyama, H.; Kishimoto, A.; Kuwabata, S. J Chem Soc Chem Commun 1991, 1986.
2. Porter, T. L.; Hagerman, M. E.; Eastman, M. P. Recent Res Dev Polym Sci 1997, 1, 1.
3. Kawaguchi, H. Prog Polym Sci 2000, 25, 1171.
4. Kalinina, O.; Kumacheva, E. Macromolecules 1999, 32, 4122.
5. Wang, Y.; Herron, N. Chem Phys Lett 1992, 200, 71.
6. Dabbousi, B. O.; Bawondi, M. G.; Onitsuka, O.; Rubner, M. F. Appl Phys Lett 1995, 66, 1316.
7. Tyan, H.-L.; Liu, Y.-C.; Wei, K.-H. Chem Mater 1999, 11, 1942.
8. (a) Wang, Z.; Pinnavaia, T. J. Chem Mater 1998, 10, 3769; (b) Biswas, M.; Ray, S.-S. Adv Polym Sci 2001, 155, 167.
9. Lan, T.; Kaviratna, P. D.; Pinnavaia, T. J. Chem Mater 1994, 6, 573.
10. Gilman, J. W.; Jackson, C. L.; Morgan, A. B.; Hayyis, R., Jr.; Manias, E.; Giannelis, E. P.; Wuthenow, M.; Hilton, D.; Phillips, S. H. Chem Mater 2000, 12, 1866.
11. (a) Yeh, J.-M.; Liou, S.-J.; Lai, C.-Y.; Wu, P.-C.; Tsai, T. Y. Chem Mater 2001, 13, 1131; (b) Yeh, J.-M.; Liou, S.-J.; Lin, C.-Y.; Cheng, C.-W.; Lee, K.-R. Chem Mater 2002, 14, 154.
12. Chandrakanthi, R. L. N.; Careem, M. A. Thin Solid Films 2002, 417, 51.
13. Wu, Q.; Xue, Z.; Qi, Z.; Wang, F. Polymer 2000, 41, 2029.
14. Lira-Gautu, M.; Gomez-Romera, P. J Solid State Chem 1999, 147, 601.
15. Jia, W.; Segal, E.; Kornemandel, D.; Lomhot, Y.; Narkis, M.; Siegmann, A. Synth Met 2002, 128, 115.
16. Roy, B. C.; Gupta, M. D.; Bhowmik, L.; Ray, J. K. J Appl Polym Sci 2002, 86, 2662.
17. Conklin, J. A.; Huang, S. C.; Huang, S. M.; Wen, T.; Kaner, R. B. Macromolecules 1995, 28, 6522.
18. Yeh, J.-M.; Chin, C.-P. J Appl Polym Sci 2003, 88, 1072.
19. Palaniappan, S. Polym Int 2000, 49, 659.
20. Gok, A.; Sari, B.; Talu, M. J Appl Polym Sci 2003, 88, 2924.
21. Ҫengeloğlu, Y.; Kır, E.; Ersöz, M. J Colloid Interface Sci 2001, 244, 342.
22. Ray, S. S. Mater Res Bull 2002, 37, 813.
23. Gruger, A.; Novak, A.; Regis, A.; Colomban, P. J Mol Struct 1994, 328, 153.
24. Biswas, M.; Ray, S. S.; Liu, Y. Synth Met 1999, 105, 99.
25. Ballav, N.; Biswas, M. Polym Int 2003, 52, 179.
26. Oriakhi, C. O.; Lerner, M. M. Mater Res Bull 1995, 30, 723.
27. Palaniappan, S.; Narayana, B. H. Polym Adv Technol 1994, 5, 225.
28. Mattoso, L. H. C.; Manohar, S. K.; Mac Diarmid, A. G.; Epstein, A. J Polym Sci Part A: Polym Chem 1995, 33, 1227.
29. Deng, J.; Ding, X.; Zhang, W.; Peng, Y.; Wang, J.; Lang, X.; Li, P.; Chen, A. S. C. Polymer 2002, 43, 2179.
30. Langer, J. J. Adv Mater Opt Electron 1999, 9, 1.
31. Chen, K. H.; Yang, S. M. Synth Met 2003, 51, 137.
32. Patil, S. F.; Bedeker, A. G.; Patil, R. C. Ind J Chem 1994, 33, 580.
33. Kim, B. H.; Jung, J. H.; Kim, J. W.; Choi, H. J.; Joo, J. Synth Met 2001, 121, 1311.
34. Kim, B. H.; Jung, J. H.; Hong, S. H.; Kim, J. W.; Choi, H. J.; Joo, J. Curr Appl Phys 2001, 1, 112.
35. Muellerleile, J. T.; Freeman, J. J. J Appl Polym Sci 1994, 54, 135.